

Influence of topological features and U^- -centers on electric charge carrying at strong electric fields in $\text{Ge}_x\text{As}_y\text{Te}_{100-x-y}$ amorphous films

A.I. Isayev¹, S.I. Mekhtiyeva¹, H.I. Mammadova¹,
R.M. Rzayev², R.I. Alekberov^{1,2}

¹Institute of Physics, Azerbaijan National Academy of Sciences,
13 G.Javid Ave., 1143 Baku, Azerbaijan

²Azerbaijan State University of Economics (UNEC), 6 Istiqlaliyyat Str.,
1001 Baku, Azerbaijan

Received September 30, 2022

As a result of studying the current-voltage characteristics of $\text{Te}-\text{Ge}_x\text{As}_y\text{Te}_{100-x-y}-\text{Al}$ structure at a negative potential of the tellurium electrode, it has been found that at applied electric field voltage exceeding $5 \cdot 10^4$ V/cm, the current-voltage dependence has the N -shape and exhibits instability in the form of irregular current oscillations. The observed features of electric charge transfer under the influence of strong electric fields are interpreted taking into account the topological features of amorphous chalcogenides and the role of U^- -centers in the process of generation and recombination of electric charge carriers in the studied structure.

Keywords: chalcogenide glass, amorphous, non-crystalline, switching effect.

Вплив топологічних особливостей та U^- -центрів на перенос електричного заряду в сильних електрических полях в аморфних плавках $\text{Ge}_x\text{As}_y\text{Te}_{100-x-y}$ А.І.Ісаєв, С.І.Мехтієва, Н.І.Маммадова, Р.М.Рзаєв, Р.І.Алекберов

Як результат дослідження вольт-амперних характеристик у структурі $\text{Te}-\text{Ge}_x\text{As}_y\text{Te}_{100-x-y}-\text{Al}$ при негативному потенціалі на телуровому електроді було встановлено, що при прикладеному потенціалі електричного поля вище за $5 \cdot 10^4$ В/см, залежність струму від напруги демонструє N -форму і нестабільність у вигляді нерегулярних осциляцій струму. Виявлені особливості переносу електричного заряду під впливом сильних електрических полів інтерпретуються з урахуванням топологічних особливостей аморфних халькогенідів і ролі U^- -центрів у процесі генерації та рекомбінації носіїв електричного заряду в досліджуваній структурі.

1. Introduction

Chalcogenide glassy semiconductors (CGS) are transparent in the infrared (IR) region of the optical spectrum and have a high refractive index. These materials are easily amenable to unlimited alloying and variation of chemical composition, which makes it possible to obtain compositions with a wide range of parameters. The noted

unique properties, as well as the functionality of CGS have been of great interest to researchers of this class of materials since the 1990s [1–9]. In 1962, the author of [10] reported the observation of a region with a negative differential resistance on the current-voltage characteristic (CVC) of the As–Te–J system, i.e. the S -shape CVC. A characteristic of this type was also observed by the authors of [11] in the Tl–As–Se(Te) sys-

tem at an applied pulsed voltage. Ovshinsky [12] observed the S-shape CVC and the memory effect in the $\text{Si}_{12}\text{Te}_{48}\text{As}_{30}\text{Ge}_{10}$ system and showed the possibility of commercial use of these materials a pronounced active area of electronic keys and memory cells, which caused an increase in the interest in this class of materials. But long-term attempts to use CGS for these purposes were not successful. The operation of the created devices was unstable and their properties deteriorated over time, which led to a gradual decrease in interest in the study of CGS. The rapid growth in the number of works devoted to the study of the effect of switching and memory in chalcogenide glasses was occurred in the 90s, when it was proposed to use the Ge–Sb–Te system in a rewritable optical disk [13]. Recently, many works have been devoted to the study of switching and memory effects in CGS materials and various mechanisms have been proposed to interpret their features. The memory effect was first observed by the author of [14] in chalcogenide glasses and explained by the transition of a substance from an amorphous state to a crystalline one, which was confirmed by other authors. However, despite the existence of numerous studies devoted to the switching effect in chalcogenide glasses, there is currently no definite mechanism that could explain all the features of this effect and further research on this problem is required. The choice of compositions consisting of three and more elements with different short-range order (SRO) parameters, as well as contacts of various types will provide information about the mechanism of current depending on the chemical composition and type of contacts.

This article is devoted to studying the effect of a strong electric field and chemical composition on the current mechanism in $\text{Te}-\text{Ge}_x\text{As}_y\text{Te}_{100-x-y}\text{Al}$ structures. The choice of the $\text{Ge}_x\text{As}_y\text{Te}_{100-x}$ glass composition as an object of the study is due to the fact that, the replacement of metallic Sb with As will allow one to obtain a material with a stronger covalent bond, which ensures its chemical stability [34]. Secondly, it is known that the electronic properties of CGS materials, including binary and complex arsenic-containing compositions, are controlled with their own charged defects with a negative correlation energy — U^- -centers; their concentration can be changed by varying the chemical composition, as well as introducing impurities, which manifests itself

in the form of charged centers [15–18, 31, 33–36]. Studies [19, 20–30] show that the topological features of the Ge–As–Se(Te) chalcogenide glass system change depend on the coordination number, which affects the electronic processes. These facts indicate that the chosen object, as well as the planned studies, will provide information on the mechanism of the influence of these factors on the current flow through the chalcogenide in the regime of a strong electric field.

2. Experimental

The synthesis of $\text{Ge}_x\text{As}_y\text{Te}_{100-x-y}$ compositions was carried out in the following sequence: highly pure elemental substances (Ge, As, Te) in the required atomic percentages were placed into quartz ampoules with an internal diameter of 12 mm; then air was pumped out to a pressure of $1.33 \cdot 10^{-4}$ Pa to prevent oxidation of the materials; then they were heated to a temperature of $\sim 900^\circ\text{C}$ during 3 hours and kept for about 12 hours at this temperature. The synthesis was carried out in a rotary furnace in order to ensure the homogeneity of samples, and cooling was carried out in the out-of-furnace mode. Films with a thickness of 3 μm used in research were obtained by thermal deposition at a rate of 0.3 $\mu\text{m}/\text{s}$ on glass substrates in vacuum at a pressure of $1.33 \cdot 10^{-4}$ Pa. $\text{Ge}_{8.33}\text{As}_{16.67}\text{Te}_{75}$, $\text{Ge}_{10}\text{As}_{20}\text{Te}_{70}$, $\text{Ge}_{12.5}\text{As}_{25}\text{Te}_{62.5}$, $\text{Ge}_{18.2}\text{As}_{18.2}\text{Te}_{63.6}$ and $\text{Ge}_{18}\text{As}_{17}\text{Te}_{55}$ glass compositions have been synthesized. The amorphous properties of the thermal evaporated films were proved by X-ray diffraction analysis on a D8-Advance powder diffractometer (Fig. 1). The amorphous state of chalcogenide glass substances was confirmed by wide maxima observed in the diffraction patterns. The current-voltage characteristic of the $\text{Te}-\text{Ge}_x\text{As}_y\text{Te}_{100-x-y}-\text{Al}$ structure has been studied in direct current by applying the voltage of both poles. Plane parallel electrodes made of aluminum and tellurium were also deposited by vacuum thermal evaporation. A tellurium layer with an area of 6.25 mm^2 and a thickness of 3 μm was deposited on a glass substrate (measured with an MII-4 optical microscope). The second electrode as a layer of aluminum with an area of 3.2 mm^2 was also deposited by thermal evaporation on the free surface of the sample.

The deposition rate and the physical parameters of the obtained layers (density and resistance) are presented in the Table.

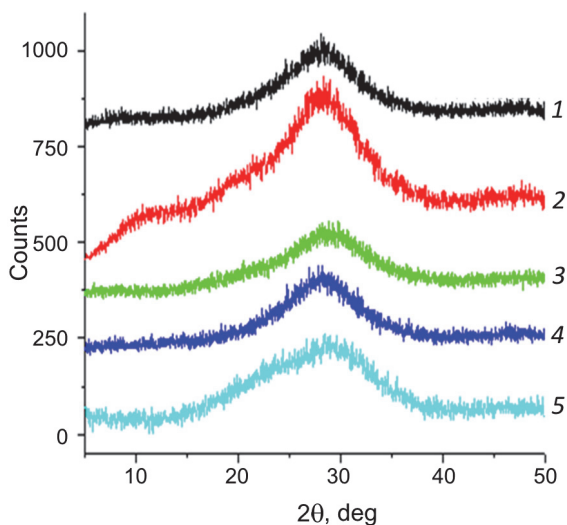


Fig. 1. X-ray diffraction patterns of Ge–As–Te chalcogenide glass compositions:
 1 — $\text{Ge}_{8.33}\text{As}_{16.67}\text{Te}_{75}$; 2 — $\text{Ge}_{10}\text{As}_{20}\text{Te}_{70}$;
 3 — $\text{Ge}_{12.5}\text{As}_{25}\text{Te}_{62.5}$; 4 — $\text{Ge}_{18.2}\text{As}_{18.2}\text{Te}_{63.6}$;
 5 — $\text{Ge}_{18}\text{As}_{17}\text{Te}_{55}$.

The choice of contacts is based on considerations that Ge–As–Te chalcogenide glass is a *p*-type semiconductor. Tellurium, also possessing *p*-type conductivity, ensures the injection of holes, i.e. main current carriers. A metallic aluminum electrode is used as an ohmic contact. Current values are recorded by a voltage source 64876 picoammeter (Keithley). The current-voltage characteristics of the samples were measured in a stationary mode.

3. Results and discussion

Fig. 2 shows *I*–*V* characteristics of $\text{Al}-\text{Ge}_x\text{As}_y\text{Te}_{100-x-y}\text{-Te}$ structure at room temperature, with positive (Fig. 2a) and negative (Fig. 2b) potentials applied to tellurium electrodes. In this case of a positive potential applied to tellurium electrode, the observed features of the curves (Fig. 2a) indicate that the transfer of electric charge is

Table. Physical parameters of deposited chalcogenide glass layers

Chemical compositions	Thermal evaporation rate, $\mu\text{m/s}$	Density, g/cm^3	Resistance, Ω
$\text{Ge}_{8.33}\text{As}_{16.67}\text{Te}_{75}$	0.3	6.22	$1.3 \cdot 10^6$
$\text{Ge}_{10}\text{As}_{20}\text{Te}_{70}$	0.3	6.01	$6.7 \cdot 10^6$
$\text{Ge}_{12.5}\text{As}_{25}\text{Te}_{62.5}$	0.3	5.14	$2.0 \cdot 10^6$
$\text{Ge}_{18.2}\text{As}_{18.2}\text{Te}_{63.6}$	0.3	6.03	$2.1 \cdot 10^6$
$\text{Ge}_{18}\text{As}_{17}\text{Te}_{55}$	0.3	5.96	$5.5 \cdot 10^6$

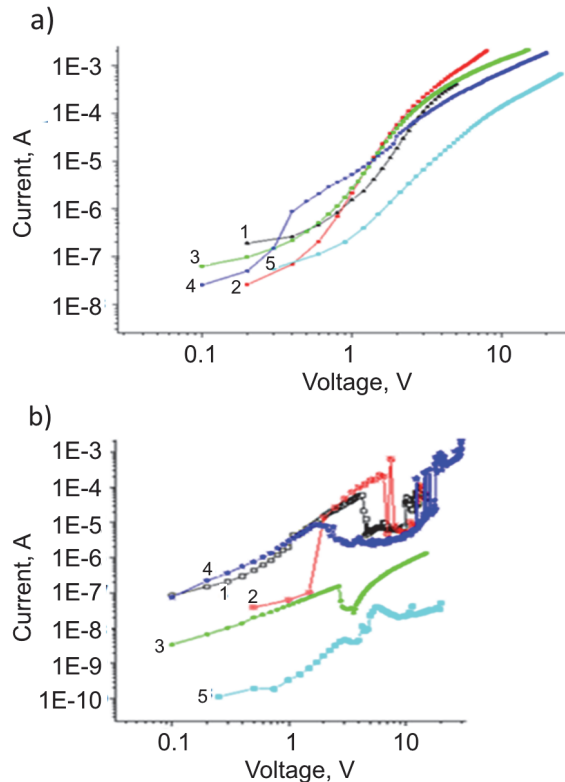


Fig. 2. *I*–*V* characteristics of the $\text{Al}-\text{Ge}_x\text{-As}_y\text{Te}_{100-x-y}\text{-Te}$ structure: positive (2a) and negative (2b) potentials applied to tellurium electrodes: 1 — $\text{Ge}_{8.33}\text{As}_{16.67}\text{Te}_{75}$;
 2 — $\text{Ge}_{10}\text{As}_{20}\text{Te}_{70}$; 3 — $\text{Ge}_{12.5}\text{As}_{25}\text{Te}_{62.5}$;
 4 — $\text{Ge}_{18.2}\text{As}_{18.2}\text{Te}_{63.6}$; 5 — $\text{Ge}_{18}\text{As}_{17}\text{Te}_{55}$.

carried out by monopolar injection currents with the participation of traps. CVCs start almost with Ohm's law, but with increasing voltage they move to power-law dependences ($I \sim V^n$, $n \approx 2$) (in this region, the value of current is proportional to the cubic thickness of sample). Further, a section with $n > 2$ is observed, which, with increasing voltage, also covers the area where $n \approx 2$. *I*–*V* characteristics of other chemical compositions almost repeat the graphs shown in Fig. 2a. The observed features of the current-voltage characteristics indicate mechanisms of the monopolar injection currents, which manifest themselves as local states located at different energy distances from the top of the valence band.

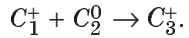
Using Lambert's classic theory of injection currents, it is established that the electricity transfer is controlled by small trap centers located between the valence band and the Fermi level. The parameters of these centers are defined by the depth of occurrence and concentration. It is shown that the current in the third region of the

CVC increases according to a power law in the region of the trap filling limit according to the Lambert theory for monoenergetic levels of hole traps. The observed feature is explained by the Pool-Frenkel effect taking into account the transition of the distribution function from the Boltzmann approximation to the Fermi-Dirac approximation, caused by a change in the position of the Fermi level [37, 38]. The critical values of electric field strength at which the thermal field of Coulomb barrier decreases down to zero blocking of the free current carriers of the thermal field are evaluated, and the magnitude of the electric field strength in the transition from the trap quadratic law to the trapless one is determined. The results mentioned above were published in our paper [15]. Therefore, in this article the current-voltage characteristics (Fig. 2b) of the structure are studied in detail when a negative potential is applied to the tellurium electrode.

As can be seen from Fig. 2b, the *I*-*V* characteristics of the structure under study when a negative potential is applied to tellurium electrode differs greatly from Fig. 2a. In this case, the current-voltage characteristic begins with a linear section, which, with increasing voltage, is replaced by a nonlinear dependence and passes into an *N*-shape region starting from an electric field of $\sim 5 \cdot 10^4$ V/cm. In some samples, an instability of the type of irregular current oscillations is observed (Fig. 2b). To understand the mechanism of electronic processes in non-crystalline materials, it would be reasonable to use the existing theoretical approaches concerning the main features of the microstructure, as well as the role of defect states in the control of electronic properties. The basic concept of the theory of electronic processes is based on the periodicity of the structure of crystals. This approach is not acceptable due to the lack of long-range order in the arrangement of atoms in non-crystalline substances. Therefore, the topological concepts are successfully applied in the interpretation of electronic properties of non-crystalline materials. Physical properties of amorphous and glassy substances are largely determined by the rigidity of the amorphous matrix. According to the topological constraint theory developed by Phillips and Thorpe [16–18], an amorphous matrix is in a flexible state when the number of degrees of freedom per atom exceeds the number of constraints in the interatomic force field. When these val-

ues are equal to the value of the average coordination number ($Z = 2.4$) there is a transition of the amorphous matrix from a flexible state to a rigid one. Thorpe [18] proposed the idea of a relationship between the rigidity of the matrix and the number of vibrational modes with zero frequency and predicted that with increasing Z , the proportion of such modes decreases and disappears at the critical value of Z ($Z = 2.4$), which leads to a decrease in rigidity. However, other studies [19–20] showed that in chalcogenide glasses, there is an intermediate phase between the flexible and stress-rigid states of the amorphous matrix [21–22], i.e. the transition from the first state to the second occurs in a certain range of Z . When studying the percolation of the structure of chalcogenide glasses, the *R*-parameter also plays an important role, which is determined by the ratio of the number of possible covalent bonds of chalcogen atoms to the number of possible covalent bonds of nonchalcogen atoms [23]. At $R = 1$, the amorphous matrix is characterized by heteropolar bonds; its stoichiometric composition $\text{Ge}_{12.5}\text{As}_{25}\text{Te}_{62.5}$ ($R = 1$; $Z = 2.50$) corresponds to the chemical threshold. Samples under study become stress-hard ($\text{Ge}_{18.2}\text{As}_{18.2}\text{Te}_{63.6}$ and $\text{Ge}_{18}\text{As}_{17}\text{Te}_{55}$ compositions) [24] as a result of the further increase in the value of Z and a decrease in R . To interpret the features of current-voltage characteristics of the structure, one should also take into account the role of charged defects with negative correlation energy (U^- -centers). As a result, a deviation from the 8–*N* rule appears as topological defects in chalcogenide glass materials, the valence requirements are not met and broken bonds occur. For example, the broken bonds arise due to destruction of Se_8 ring molecules in selenium (Se). In addition, defects of this type also exist at the ends of long chain molecules. Each broken bond containing one electron is also electrically neutral. A broken bond with a defect is denoted as C_1^0 . Based on the idea by Anderson [26] about a strong electron-phonon interaction, Street and Mott [25] suggested that a broken bond without an electron or with two electrons is energetically more favorable than two states of the C_1^0 type. These states are denoted as C_1^+ , C_1^- . The existence of these defects in high concentrations in these materials is confirmed by the fact that the Fermi level is fixed in the middle of the band gap, as well as by the study of photoluminescence and conductivity in an alternating electric

field. In the models proposed by the authors of [27], U^- -centers are considered as defects, which are predominantly in the C_3^+ and C_1^- -states, which are called valence alternation pair (VAP). The triply coordinated C_3^+ defect promotes the interaction between the positively charged end of a dangling bond without electrons and the lone pair of electrons of neighboring chain molecules [28].



To explain the switching effect in the Ge-Sb-Te system, a mechanism was proposed based on the thermal field ionization of U^- -centers and the capture of charge carriers by them [7, 29]. Taking into account that the energy of the main state of negative U^- -centers is several tens of electron volts, we believe that thermoionization and capture of charge carriers is a multiphonon process. The theory of multiphonon tunneling ionization of deep centers was developed by authors [30–33]. We believe that the features of current-voltage characteristics observed by us in the structure under study are also associated with the processes of multiphonon thermal field ionization of U^- -centers and capture of charge carriers. As can be seen from Fig. 2b, the $I196V$ characteristic of the $\text{Al}-\text{Ge}_x\text{As}_y\text{Te}_{100-x-y}-\text{Te}$ structure at a negative potential at the tellurium electrode begins with a linear law, while at the electric field voltage of $\sim 10^4$ V/cm, this law is replaced by a nonlinear dependence of current on applied voltage; but at the value of $2 \cdot 10^4 \div 10^5$ V/cm, the current decreases sharply with increasing voltage, i.e. we observe the N -shape region, and chalcogenide glass compositions pass into a high-resistivity state. Finally, in the last section of the I-V characteristic, the dependence corresponding to the low-resistance state is observed. It is assumed that the section of the $I196V$ characteristic starting from the electric field strength of $\sim 5 \cdot 10^3$ V/cm is associated with the release of charge carriers from shallow local states. Ionization of U^- -centers begins with an increase in the electric field strength; as a result, at a certain field strength, when the concentration of free charge carriers reaches a critical value, an avalanche-like capture of carriers by U^- -centers occurs or recombination of electrons and holes, which is accompanied by a sharp increase in the resistivity of the sample. The observed instability as irregular oscillations in the $I196V$ characteristics with an N -shape re-

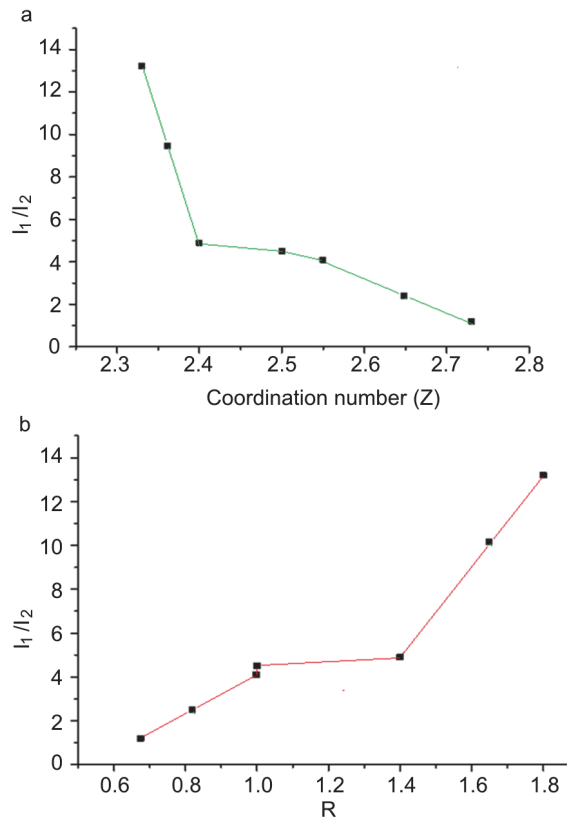


Fig. 3. Dependence of I_1/I_2 on the average value of the coordination number (Z) (3a) and on the parameter R (3b) in the N -shape re-

gion is apparently associated with periodically repeating processes of ionization of U^- -centers and capture of charge carriers by these centers. The probability of capture of charge carriers is greatly reduced at high electric field voltages and again the resistivity of samples decreases. With a positive potential at the tellurium electrode, the strong injection of charge carriers prevails over the processes of ionization and trapping; and in this case, there is no an N -shape region in the $I196V$ characteristics (Fig. 2a).

Fig. 3 shows the dependence of I_1/I_2 on the average value of the coordination number Z (3a) and on the parameter R (3b) in the N -shape region of I-V characteristics, where I_1 is the current in the low-resistance region and I_2 is the current in the high-resistance region.

It can be seen that with an increase in Z or decrease in R , the ratio of I_1/I_2 decreases in the area, where Z increases from 2.4 to 2.55 and R decreases from 1.4 to 0.998. This is explained by the fact that the indicated range of Z and R corresponds to an isostatically rigid state, in which a grad-

ual transition of a substance from a labile, flexible structure to a stressed-rigid state occurs [24]. The observed features of the current-voltage characteristics for studied structures indicate a significant role of topological features in the processes of electric charge transfer. Taking into account that the electric charge transfer in chalcogenide glasses is controlled by U^- -centers, we can assert that their concentration is controlled by topological features. The changes in the numerical values of I_1/I_2 depending on the chemical composition can be associated with the changes in the concentration of U^- -centers. In this case, the accumulation of U^- -centers is expected in samples with a high concentration of tellurium atoms (where $Z < 2.4$; $R > 1$). The proportion of Te–Te chemical bonds is quite high [24] in the indicated chalcogenide glass compositions and their low binding energy contributes to the breaking of this bond; this leads to an increase in the number of dangling bonds and the concentration of U^- -centers associated with them (pairs with alternating valence C_3^+ and C_1^- increase in the value of Z and a decrease in R are accompanied by an increase in the proportion of chemical bonds with high binding energies (Ge–Te, As–Te) [24], which cause a decrease in the concentration of dangling bonds (U^- -centers). As a result, there is strong decrease in the value of I_1/I_2 (Fig. 3) and disappearance of instability in samples with high Z -values and low R -values ($Ge_{12.5}As_{25}Te_{62.5}$, $Ge_{18}As_{17}Te_{55}$). These results show that the creation of U^- -centers is associated with appearance of dangling bonds in glass materials under study.

4. Conclusion

It has been shown that the current-voltage characteristics of the $Al-Ge_xAs_yTe_{100-x-y}-Te$ structure, with a negative potential at the tellurium electrode, at the strength of applied electric field exceeding $\sim 5 \cdot 10^3$ V/cm exhibit a non-linear character, and N-shape dependences are observed at field strengths in the range of $2 \cdot 10^4 \div 10^5$ V/cm. It is assumed that the nonlinear region of the current-voltage (IV) characteristics is associated with field depletion of shallow local levels, and the N-shape range of the characteristics is due to the processes of multiphonon thermal field ionization of U^- -centers and capture of charge carriers by these centers. Irregular oscillations at the current-voltage characteristics are associated with periodically repeating processes of

ionization of IU^- -centers and capture of charge carriers. A strong decrease in the ratio of currents (I_1/I_2) in the N-shape characteristic region with an increase of the coordination number and a decrease in the parameter R , i.e. the transition from labile to hard state, is associated with a decrease in the lower energies bonds (Te–Te) and an increase in the bonds with a high binding energy (Ge–Te, As–Te).

References

1. K.D.Tsendin, Electronic Phenomena in Chalcogenide Glassy Semiconductors, Science, Moscow (1996).
2. K.Tanaka, K.Shimakawa, Amorphous Chalcogenide Semiconductors and Related Materials, Springer (2011).
3. A.Zakery, S.Elliott, *Journal of Non-Crystalline Solids*, **330**, 1 (2003).
4. J.S.Sanghera, I.D.Aggarwal, *Journal of Non-Crystalline Solids*, **256–257**, 6 (1999).
5. T.Wang, O.Gulbiten, R.P.Wang et al., *Journal of Physical Chemistry B*, **118**, 1436 (2014).
6. M.Nardone, M.Simon, I.V.Karpov, V.G.Karpov, *Journal of Applied Physics*, **112**, 071101 (2012).
7. N.A.Bogoslovsky, K.D.Tsendin, *FTP*, **46**, 577 (2012).
8. N.Chandel, N.Mehta, *J.of Physics and Chemistry of Solids*, **115**, 113 (2018).
9. R.T.A.Kumar, S.T.Mahmouda, D.P.Padiyanb, N.Qamhieha, *Optik*, **152**, 1 (2018).
10. A.D.Pearson, W.R.Northover, I.F.Dewald, I.W.Peek, Advance in Glass Technology, Plenum Press (1962).
11. B.T.Kolomiets, E.A.Lebedev, *Radio Engineering and Electronics*, **8**, 2097 (1963).
12. S.R.Ovshinsky, *Phys.Rev.Lett.*, **21**, 1450 (1968).
13. N.Yamada, E.Ohno, K.Nishiuchi et al., *J. Appl.Phys.*, **69**, 2849 (1991).
14. S.R.Ovshinsky, *J.Non-Cryst.Sol.*, **2**, 99 (1970).
15. H.I.Mammadova, *AJP Fizika*, **25**, 52 (2019).
16. J.C.Phillips, *J.Non-Crystalline Solids*, **34**, 153 (1979).
17. C.Phillips, M.F.Thorpe, *Solid State Commun.*, **53**, 699 (1985).
18. Thorpe, *J. Non-Crystalline Solids*, **57**, 355 (1983).
19. P.Boolchand, X.Feng, W.J.Bresser, *J.Non-Crystalline Solids*, **293–295D**, 348 (2001).
20. D.G.Georgiev, P.Boolchand, M.Micoulaut, *Physical Review*, **62**, 9228 (2000).
21. J.C.Phillips, *Physical Review B*, **88**, 216401 (2002).
22. M.Micoulaut, J.C.Phillips, *Physical Review*, **67**, 104204 (2003).
23. L.Tichy, H.Ticha, *Mater.Lett.*, **21**, 313 (1994).

-
24. A.I.Isayev, H.I.Mammadova, S.I.Mekhtieva, R.I.Alekberov, *FTP*, **54**, 1052 (2020).
25. R.A.Street, N.F.Mott, *Phys. Rev. Lett.*, **35**, 1293 (1975).
26. P.W.Anderson, *Phys. Rev. Lett.*, **34**, 953 (1975).
27. M.Kastner, D.Adler, H.Fritzsche, *Phys. Rev. Lett.*, **37**, 1504 (1976).
28. A.V.Kolobov, J.Tominaga, Chalcogenides, Springer-Verlag Berlin Heidelberg (2012).
29. N.A.Bogoslovsky, K.D.Tsendin, *FTP*, **43**, 1878 (2009).
30. V.N.Abakumov, I.A.Merkulov, V.I.Perel, I.N.Yassievich, *JETF*, **89**, 1472 (1985).
31. V.Karpus, V.I.Perel, *JETF*, **42**, 403 (1985).
32. V.Karpus, V.I.Perel, *JETF*, **91**, 2319 (1986).
33. V.N.Abakumov, V.Karpus, V.I.Perel, I.N.Yassievich, *FTP*, **22**, 262 (1988).
34. L.P.Kazakova, E.A.Lebedev, N.B.Zakharova et al., *J. of Non-Crystalline Solids*, **167**, 65 (1994).
35. R.I.Alekberov, A.I.Isayev, S.I.Mekhtiyeva, M.Fabian, *Physica B: Condensed Matter*, **550**, 367 (2018).
35. R.I.Alekberov, S.I.Mekhtiyeva, A.I.Isayev, M.Fabian, *J. Non-Crystalline Solids*, **470**, 152 (2017).
35. J.Frenkel, *Physical Review*, **54**, 647 (1938).
35. W.R.Harrell, Poole-Frenkel Conduction in Silicon Dioxide Films, and Implications for Hot-Carrier Degradation in *n*-MOS Devices, Doctoral Dissertation, University of Maryland (1994).